Redox-driven exsolution of iron-titanium oxides in magnetite in Miller Range (MIL) 03346 nakhlite:

Evidence for post crystallization oxidation in the nakhlite cumulate pile?

MS 4926 Revision 2

K. Righter[1]

L.P. Keller[2]

Z. Rahman[3],

R. Christoffersen[3]

[1]NASA JSC, Mailcode KT, 2101 NASA Pkwy., Houston, TX 77058; kevin.righter-1@nasa.gov),

[2]NASA-JSC, Mailcode KR,

[3]ESCG Jacobs, Houston, TX.

Abstract – The Miller Range (MIL) 03346 nakhlite contains ~20% mesostasis which contains skeletal titanomagnetite. The titanomagnetite contains trellis-type {111} lamellae of ilmenite similar to those found in terrestrial titanomagnetites that have experienced subsolidus redox reactions during cooling of their host rocks. We have characterized the MIL 03346 titanomagnetite-ilmenite intergrowths by a combination of focused ion beam (FIB), energy dispersive spectroscopy (EDX), and high resolution transmission electron microscopy (TEM). The resulting structural and chemical analyses have been combined with temperature and fO_2 data from previous studies of MIL 03346, as well as previous work on two-oxide thermobarometry of nakhlites. Our calculations show that as MIL 03346 and other nakhlites cooled below 800 ºC, they recorded increasingly reducing conditions, such that the lowest temperatures calculated correspond to fO_2 conditions as low as 4 log fO_2 units below the FMQ buffer. However, the MIL 03346 lamellae must have formed by oxidation and thus record a very late stage low temperature (<350 ºC) oxidation event. When considered together with previous studies of MIL 03346 and nakhlites in general, the overall cooling history could be explained by early oxidation followed by intermediate stage reduction caused by S_2 loss by degassing, followed by late loss of Cl by degassing.

Introduction

Our understanding of the geologic history of Mars has been revolutionized by studies of meteorites that originated from that planet (McSween, 2008). From these detailed studies we have learned the precise ages, chemical compositions, mineralogy, alteration history, volatile contents and magmatic history of a diverse suite of samples, including basalts, pyroxenites, and ultramafic rocks (McSween, 2008). In particular, the magmatic history is constrained by the shergottites which range in age from 575 to 150 Ma and nakhlites which have ages near 1.3 Ga. Studies of these two groups have led to a detailed understanding of magma genesis that includes generation of basalt by melting of the martian mantle (e.g., Filiberto et al., 2008; Monders et al., 2007; Musselwhite et al., 2006), fractionation of primitive melts to form basalt (Symes et al., 2008), and the generation of nakhlites by crystallization and accumulation of pyroxene and olivine from a basaltic parental melt (Treiman, 2005).

Oxygen fugacity (fO_2) is an important magmatic variable that controls phase equilibria and also defines mantle-crust-atmosphere interactions. The fO_2 at which shergottites and nakhlites formed has been determined by many detailed studies of individual meteorite samples; shergottites define a range from near the iron-wustite (IW) buffer to just below the fayalite-magnetite-quartz (FMQ) buffer (Goodrich et al., 2003; Herd et al., 2002; McCanta et al., 2004), whereas nakhlites are typically more oxidized near FMQ (McCanta et al., 2004; 2009; Bunch and Reid, 1975; Szymanski et al., 2010; Hammer, 2009; Rutherford and Hammer, 2008, Herd and Walton, 2008; Treiman and Irving, 2008; Sautter et al. 2002). Nakhlites are the most oxidized samples, and it is important to understand what produces the high end of the fO_2 range. There have been many approaches to studying and understanding nakhlite fO_2, including pyroxene Fe and REE contents (McCanta et al., 2004; 2009), two oxide barometry (Bunch and Reid,

1975; Szymanski et al., 2010), and experimental petrology (Hammer, 2009; Rutherford and Hammer, 2008, and Herd and Walton, 2008). Despite the many studies there are a range of fO_2 values measured using the different approaches and a fundamental understanding of the variation has been elusive. Studies of Fe-Ti oxides in nakhlites have led to additional constraints on their equilibration temperatures and fO_2s (Bunch and Reid, 1975; Treiman and Irving, 2008; Szymanski et al., 2010; Sautter et al. 2002), but even this approach has led to a range of fO_2 values and temperatures from 500 to 1000 ºC.

Among the nakhlites, the Miller Range (MIL) 03346 pairing group is recognized as among the most oxidized, and may represent the top-most sample in a small or shallow magmatic body. MIL 03346 is one of the most mesostasis-rich nakhlites (Treiman, 2005) and thought to have equilibrated at oxygen fugacities near the FMQ buffer (Righter et al., 2008; Dyar et al., 2005). The MIL 03346 mesostasis contains skeletal titano-magnetite, but does not contain coarse-grained magnetite and ilmenite crystals as do many of the other nakhlites, and so this sample has not been part of the two oxide barometry studies.

However, several scientists (e.g. Makashima et al., 2007) have noted that this titano-magnetite contains very fine exsolution lamellae (Figure 1). Moreover, the lamellae are so small that they cannot be characterized by electron microprobe analysis (EMPA) or other standard approaches. The trellis-type lamellae typically form by oxidation (Haggerty, 1976), so studies of the oxide and the lamellae formation may offer some new constraints on the origin of the fO_2 variation within nakhlites and within the martian meteorite suite in general. Here we report the first characterization of the mineralogy of the lamellae phase. We select several areas for focused ion beam (FIB) extraction, prepare transmission electron microscopy (TEM) foils, and identify and

analyze the lamellae using TEM. The resulting analyses are combined with previous work on nakhlites to interpret the thermal and oxidation history of this meteorite group.

SEM petrography and FIB extraction

Several regions of MIL 03346 (,106) where well developed lamellae are present in grains thick enough with depth to support FIB sectioning (Fig. 1), were identified by scanning electron microscopy (SEM). The lamellae are no more than 2 μm thick, and form a trellis-like pattern oriented on the {111} crystallographic planes of the host titanomagnetite. The intergrowth is typical of so-called "oxy-exsolved" titanomagnetites described from a range of terrestrial rocks, particularly basalts (Haggerty, 1976). Regions within the host titanomagnetite containing the lamellar intergrowths were extracted in the form of 1 x 10 x 15 μm sections (Fig. 1) using a dual focused ion-beam **(**FIB) instrument (FEI: Quanta 3D-FEG) using 30 kV Gallium ion-beam at the NASA Johnson Space Center (JSC) and then thinned further using 5 kV and 2 kV gallium ions for TEM work (Fig. 1).

EDX data and TEM analysis

We obtained imaging, diffraction and chemical data from the FIB section using the NASA-JSC JEOL 2500 field-emission STEM equipped with a Noran thin window energy-dispersive X-ray (EDX) spectrometer. Calculation of Fe_2O_3 and FeO proportions was done using charge balance and stoichiometry and demonstrates that the exsolved magnetite is nearly pure Fe_3O_4 component (Table 1). The magnetite contains only a small amount of Al and Ti. In addition, the ilmenite has a Mg/Mn ratio of 0.126, and the magnetite has a very low Mg/Mn ratio of < 0.128. These similar values suggest equilibration was approached, as defined by Bacon and Hirschmann

(1988) (Table 1). From the EDX analyses, the ilmenite stoichiometry is ~$(Fe_{0.97}Mn_{0.03})TiO_3$. The host titano-magnetite is $(Fe_{2.76}Al_{0.13}Ti_{0.11})O_4$. When Fe^{2+} and Fe^{3+} in magnetite and ilmenite lamellae are calculated based on charge balance and stoichiometry (Table 1), and Fe^{2+}, Fe^{3+} and Ti are plotted on a ternary diagram, it is clear that oxidation has occurred in the host magnetite (see equation 2 below), causing the exsolution that is expected in trellis-type exsolution features (Figure 2). The tie line between ilmenite (green) and magnetite falls to the right of the original bulk composition (yellow) indicating an overall gain in Fe^{3+}, and thus oxidation; because the ilmenite contains essentially no Fe^{3+}, the remaining magnetite must contain more Fe^{3+} than the original titano-magnetite, as indicated on Figure 2.

TEM diffraction and imaging analysis confirm that the lamellae are typical trellis type oxidation-driven exsolution of ilmenite on {111} of the host titano-magnetite (Figure 3a). The high-resolution TEM image of the magnetite-ilmenite interface shows the orientation relationship (0001) Ilm ‖ (111) mag (Fig. 3b). In addition to the trellis-type oxyexsolution, there is further true subsolidus exsolution within the host titanomagnetite into nearly pure endmember magnetite $[(Fe_{2.87}Al_{0.06}Ti_{0.07})O_4]$ and more Al and Ti-rich very thin, wormy (~10 nm thick) lamellae of composition $[(Fe_{2.41}Al_{0.33}Ti_{0.26})O_4]$ exsolved on (100) (Figure 4). The Al- and Ti-rich magnetite also occurs as a ~5-10 nm thick layer at magnetite-ilmenite interfaces (not shown). An additional microstructural feature identified by TEM imaging consists of 10-20 nm size grains of hercynitic spinel ($FeAl_2O_4$) occurring at the junction of some ilmenite lamellae. (bright spot of upper right corner of Fig. 3a). The hercynite is in contact with the host titanomagnetite as well as the ilmenite lamellae. The hercynite is ~$Hrc_{86}Mt_{14}$, but contains percent levels of Zn and trace but detectable Ti and Mn. This pair of hercynite and magnetite compositions form at ~500-600 ºC , according to the Hy-Mt solvus of Turnock and Eugster (1962).

Temperature and fO_2 calculations

Equilibrium between rhombohedral (rhm) and spinel structured (spn) oxides may help constrain the conditions at which the lamellae formed. The coexistence of ilmenite and magnetite allows calculation of T and fO_2 of equilibration based on the exchange (1) and redox (2) equilibria (Buddington and Lindsley, 1964):

1) $Fe_2O_3 + Fe_2TiO_4 = FeTiO_3 + Fe_3O_4$
rhm, spn, rhm, spn,
hem. ulvosp. ilm. magnt.

2) $6\,Fe_2O_3 = 4\,Fe_3O_4 + O_2$
rhm, spn,
hem. magnt. gas

where hem. = hematite, ilm. = ilmenite, ulvosp.=ulvospinel, and magnt.=magnetite). Two versions of this geothermometer will be used here: a) the most recent version of this geothermometer, Ghiorso and Evans (2008), is best calibrated for long and short range cation order, and also includes the newest experimental data for the $Fe^{2+}Ti - (Fe^{3+})_2$ exchange equilibria, and b) the model of Ghiorso and Sack (1991) which has been widely applied to igneous rocks. Using compositions in Table 1, T and fO_2 were calculated using these geothermometers, and resulted in extremely low temperatures (~203-228°C; Table 1). These results suggest that the T- fO_2 equilibration conditions were at low temperatures but the results are outside of the reliable calibration range of the geothermometers (~ 350 °C; Ghiorso and Sack, 2008), and thus the two oxides do not, unfortunately, accurately record T- fO_2 conditions of equilibration. Additionally, the results yield relative fO_2 of ΔFMQ = -9.0, which is ~ 5.5 log fO_2

156 units below the IW buffer, where Fe metal is stable. This is also a nonsensical results because no
157 Fe metal has been observed here, and in fact oxidation of titano-magnetite is observed.
158 The exsolution of hercynite ($FeAl_2O_4$) from the titanomagnetite host is consistent with tempera-
159 tures of 500- 600 °C, based on the Turnock and Eugster (1962) solvus. Although the tempera-
160 tures derived from the two-oxide geothermometry may not be accurate because they are outside
161 the calibration range of the T-fO_2 oxybarometer/thermometers, the temperatures are nonetheless
162 all consistent with a low temperature stage in the history of MIL 03346.

163 **Comparison of MIL 03346 two oxide T and fO_2 to other nakhlites**

164 The temperatures we have determined based on the compositional relations in the MIL 03346
165 titanomagnetite-ilmenite intergrowths are quite a bit lower than many previous calculations of
166 temperature for nakhlites, and appear to be the lowest so far measured for all nakhlites (e.g.,
167 Bunch and Reid, 1975; Treiman and Irving, 2008; Szymanski et al., 2010; Sautter et al. 2002,
168 Boctor et al., 1976). Given these unusual values, we have calculated T and fO_2 for all available
169 nakhlites using chemical analyses of magnetite and ilmenite from nakhlites reported in the litera-
170 ture, using the Ghiorso and Evans (2008) Fe-Ti two-oxide geothermometer. The calculated
171 temperatures for these nakhlites (Nakhla, Lafayette, NWA 998, Yamato 000589) are higher than
172 those inferred for MIL 03346, but all the data define a trend with the lowest temperature Fe-Ti
173 pairs also being the most reduced relative to FMQ. Because MIL 03346 records a low tempera-
174 ture, and also clear evidence for oxidation, it appears that MIL 03346 would record a change in
175 the overall nakhlite trend to a set of lower-temperature, more oxidized conditions (Figure 5).
176

177 **Temperature and fO_2 history of MIL 03346 and origin of reduction and oxidation trends**

One possible explanation for the reduction trend is a reduction reaction such as $4Fe_2O_3 + S_2 = 8FeO + 2SO_2$, which occurs while SO_2 is lost through cooling and degassing. This hypothesis could be tested against careful studies of the S content of nakhlite mesostasis to see if there is a trend with the temperatures and ΔFMQ values calculated here. Although such data have not yet been obtained for MIL 03346, they have been for other nakhlites. For example, nakhlites that are thought to have formed at the shallowest depths – e.g. NWA 817 (Sautter et al., 2002) – have the lowest S contents (Chevrier et al., 2011), whereas those thought to have formed deeper – e.g. NWA 998 (Mikouchi et al., 2006) – have the highest S contents (Chevrier et al., 2011). This suggests that the shallower samples lost more S and became more reduced, whereas those forming deeper stayed oxidized and retained more S during cooling. Such a trend of temperature and ΔFMQ is observed in terrestrial volcanic tuffs such as the Bishop Tuff and Katmai and various plutons (Ghiorso and Evans, 2008; Frost and Lindsley, 1992), suggesting that there was reduction upon subsolidus cooling and degassing of those igneous bodies.

The late oxidation trend, on the other hand, could be due to loss of Cl during degassing. Cl is known to remain soluble in magma to lower pressures and temperatures than S_2, and thus degas at later stages of magmatic history (Webster et al., 1999). Once Cl degasses (as $FeCl_2$) the magma is depleted of FeO and thus magma may become oxidized (Bell and Simon, 2012):

$FeO\ (melt) + HCl\ (fluid) = FeCl_2\ (fluid) + H_2O\ (melt)$.

Martian magmas are known to contain Cl and S, and this hypothesis could help to explain the late oxidation recorded in the shallow MIL 03346 nakhlite. Indeed, McCubbin et al. (2013) document changes in apatite chemistry (MIL nakhites have higher F) that are consistent with Cl degassing at a late stage. The presence of F-rich apatites indicates that Cl and H_2O were lost earlier

(McCubbin et al., 2013; Ustunisik et al., 2011). The overall effect of degassing on S, Cl, and fO_2 is discussed in more detail in the next section.

Overall T-fO_2 history of MIL and other nakhlites

There have been many studies of the temperature and fO_2 of the MIL 03346 nakhlite, with a range of temperatures and fO_2's reported, depending on the approach taken. Here we compare our results to those of previous studies and show that the MIL nakhlite may preserve part of a cooling history that includes early oxidation, intermediate reduction, and late oxidation. The experimental textural and pyroxene compositional studies of Rutherford and Hammer (2008) indicate that the MIL nakhlites may have equilibrated at 1140 ºC and FMQ-2, whereas the Eu partitioning in pyroxene records FMQ-1 (McCanta et al., 2009), and the groundmass contains fayalite-rich olivine, magnetite, and SiO_2-rich glassy mesostasis that must have equilibrated near FMQ. Rutherford and Hammer (2008) propose that this cooling and slight oxidation trend can be explained by crystallization of the MIL nakhlite system, which was accompanied by Fe^{3+} enrichment in the liquid, thus causing slight oxidation (Figure 6). This general idea is consistent with the results of Righter et al. (2008) who calculate FMQ+0.5 and 1100 ºC based on pyroxene and melt equilibria (Figure 6). Additionally the studies of Herd and Walton (2008) are also consistent with this scenario, as well as a proposed 3 to 6 ºC/hr cooling rate. Such an oxidation trend with crystallization has been documented in terrestrial basaltic systems such as Carmichael and Ghiorso (1990) and Christie et al. (1986), and was suggested for the nakhlites by Treiman (2005). That the redox conditions were changing during the crystallization or cooling of the nakhlite magma bodies is indicated by zoning or gradients in some mineral phases (e.g., Treiman and Irving, 2008; Domeneghetti et al., 2013), as well as documentation of the sulfide-sulfate

transition in a melt inclusion from MIL 03346 (McCubbin et al., 2009). This general history of early oxidation may be quite typical for martian magmas, since most underwent fractionation (thus building up Fe^{3+} in residual liquids), as documented in LAR 06319 by Peslier et al. (2010).

Following this cooling and oxidation trend from ~1200 to 1100º C, the MIL nakhlites and nakhlites in general must have undergone additional cooling accompanied by reduction, as demonstrated in the previous section (see Fig. 6). Many may have cooled while also losing S_2 gas causing the late stage reduction. In contradistinction to the nakhlites, the oxidation trend from 1200 to ~750 ºC seen in LAR 06319 (Peslier et al., 2010), may be a case where there was limited degassing until temperatures lower than 750 ºC. Finally, the late loss of Cl from MIL 03346 during further cooling and degassing may have caused late oxidation of the magnetite in the shallowest portion of the nakhlite magmatic system (Fig. 6).

Implications

The nakhlites may thus document the early oxidation seen in some shergottites, followed by later reduction with S_2 degassing, followed by later oxidation caused by Cl degassing. This idea is supported by the fact that the most shallow nakhlites also contain the least S and Cl (Chevrier et al., 2011; McCubbin etal., 2013), the most oxidized samples are near the top (Mikouchi et al., 2006; McCubbin et al., 2013), and the most reduced are at the bottom (McCubbin et al., 2013; Treiman et al., 2007). This protracted cooling path of oxidation followed by reduction followed by late stage oxidation must be well understood in any magmatic system or suite of rocks from Mars before individual fO_2 calculations for any given sample can be accurately interpreted. Pulling a fO_2 value out of context may lead to erroneous conclusions regarding the magmatic fO_2 of the samples.

Acknowledgements

This research was supported by an RTOP to KR from the Mars Fundamental Research program at NASA. We thank the Meteorite Working Group for allowing the use of the thin section (,106) in this study. We also thank Associate Editor S. Simon for his comments and reviewers J. Karner and C. Herd for their reviews, all of which helped clarify the presentation of this information.

References

Bacon, C. R., & Hirschmann, M. M. (1988). Mg/Mn partitioning as a test for equilibrium between coexisting Fe-Ti oxides. American Mineralogist, 73, 57-61.

Bell, A.S. and Simon, A. (2012) Experimental evidence for the alteration of the $Fe^{3+}/\Sigma Fe$ of silicate melt caused by the degassing of chlorine-bearing aqueous volatiles. Geology, 39, 499–502.

Boctor, N.Z., Meyer, H.O.A., and Kullerud, G. (1976) Lafayette meteorite - Petrology and opaque mineralogy. Earth and Planetary Science Letters, 32, 69–76.

Buddington A. F. and Lindsley D. H. (1964) Iron-titanium oxides minerals and synthetic equivalents. Journal of Petrology, 5, 310–357.

Bunch T.E. and Reid A.M. (1975) The nakhlites, part 1: Petrography and mineral chemistry. Meteoritics, 10, 303-315.

Carmichael, I.S.E. and Ghiorso, M.S. (1990) The effect of oxygen fugacity on the redox state of natural liquids and their crystallizing phases. *in* "Modern methods of igneous petrology:

Understanding magmatic processes", J. Nicholls & J.K. Russell, eds., Mineralogical Society of America, Reviews in Mineralogy, 24, 191–212.

Chevrier, V., Lorand, J.-P. and Sautter, V. (2011) Sulfide petrology of four nakhlites: Northwest Africa 817, Northwest Africa 998, Nakhla, and Governador Valadares. Meteoritics and Planetary Science, 46, 769–784.

Christie, D.M., Carmichael, I.S.E., and Langmuir, C.H. (1986) Oxidation states of mid-ocean ridge basalt glasses. Earth and Planetary Science Letters, 79, 397-411.

Day, J.M.D., Taylor, L.A., Floss, C., and McSween, H.Y., Jr. (2006) Petrology and chemistry of MIL 03346 and its significance in understanding the petrogenesis of nakhlites on Mars. Meteoritics and Planetary Science, 41, 581–606.

Domeneghetti, M.C., Fioretti, A.M., Cámara, F., McCammon, C., and Alvaro, M. (2013) Thermal history of nakhlites: A comparison between MIL 03346 and its terrestrial analogue Theo's flow. Geochimica et Cosmochimica Acta, 121, 571-581.

Dyar, M.D., Treiman, A.H., Pieters, C.M., Hiroi, T. and Lane, M.D. (2005) MIL03346, the most oxidized Martian meteorite: A first look at petrography, mineral chemistry, and spectroscopy. Journal of Geophysical Research, 110(E9): E09005.

Filiberto, J., A.H. Treiman, and L. Le (2008) Crystallization Experiments on a Gusev Basalt Composition. Meteoritics and Planetary Science, 43, 1137-1146.

Frost, B.R. and Lindsley, D.H. (1992) Equilibria among Fe–Ti oxides, pyroxenes, olivine, and quartz. 2. Application. American Mineralalogist, 77, 1004-1020.

Ghiorso, M.S. and Evans, B.W. (2008) Thermodynamics of Rhombohedral Oxide Solid Solutions and a Revision of the Fe-Ti Two-Oxide Geothermometer and Oxygen-Barometer. American Journal of Science, 308, 957-1039.

Ghiorso, M.S., and Sack, R.O. (1991) Fe-Ti oxide geothermometry: Thermodynamic formulation and the estimation of intensive variables in silicic magmas. Contributions to Mineralogy and Petrology, 108, 485-510.

Goodrich, C.A., C.D.K Herd, and L.A. Taylor (2003) Spinels and oxygen fugacity in olivine-phyric and lherzolitic shergottites. Meteoritics & Planetary Science, 38, 1773-1792.

Haggerty, S. E (1976) Oxidation of opaque mineral oxides in basalts, in Rumble, D. (ed.) Oxide Minerals, Reviews in Mineralogy, 3, Hg1-Hg100.

Hammer, J.E. (2009) Application of a textural geospeedometer to the late-stage magmatic history of MIL 03346. Meteoritics and Planetary Science, 44, 141–154.

Herd, C.D.K. and Walton, E.L. (2008) Cooling and Crystallization of the Miller Range 03346 Nakhlite: Insights from Experimental Petrology and Mineral Equilibria. Lunar Planet. Sci. XXXIX, Abstract #1496, Lunar Planet. Inst., Houston (CD-ROM).

Herd, C.D., Borg, L.E., Jones, J.H., & Papike, J.J. (2002) Oxygen fugacity and geochemical variations in the Martian basalts: Implications for Martian basalt petrogenesis and the oxidation state of the upper mantle of Mars. Geochimica et Cosmochimica Acta, 66, 2025-2036.

Makishima J., McKay G., Le L., Miyamoto M. and Mikouchi T. (2007) Oxidation state of nakhlites as inferred from Fe-Ti oxide equilibria and augite/melt europium partitioning. Lunar and Planet. Sci., XXXVIII, Abstract #1834, Lunar Planet. Inst., Houston (CD-ROM).

McCanta, M. C. Dyar, M. D. Rutherford, M. J. Delaney, J. S. (2004) Iron partitioning between basaltic melts and clinopyroxene as a function of oxygen fugacity. American Mineralalogist, 89, 1685-1693.

McCanta, M.C., Elkins-Tanton, L.T., and Rutherford, M.J. (2009) Expanding the application of the Eu-oxybarometer to the lherzolitic shergottites and nakhlites: Implications for the oxida-

313 tion state heterogeneity of the Martian interior. Meteoritics and Planetary Science, 44, 725–
314 745.
315 McCubbin, F.M., Tosca, N.J., Smirnov, A., Nekvasil, H., Steele, A., Fries, M., Lindsley, D.H.
316 (2009) Hydrothermal jarosite and hematite in a pyroxene-hosted melt inclusion in martian
317 meteorite Miller Range (MIL) 03346: Implications for magmatic-hydrothermal fluids on
318 Mars. Geochimica et Cosmochimica Acta, 73, 4907-4917.
319 McCubbin, F.M., Elardo, S.M., Shearer, C.K., Smirnov, A., Hauri, E.H., and Draper, D.S. (2013)
320 A petrogenetic model for the comagmatic origin of chassignites and nakhlites:Inferences
321 from chlorine-rich minerals, petrology, and geochemistry. Meteoritics and Planetary Science,
322 48, 819-853.
323 McSween H. Y. (2008) Martian meteorites as crustal samples. In The Martian Surface: Composi-
324 tion, Mineralogy, and Physical Properties, J. F. Bell III editor, Cambridge University Press,
325 Cambridge, pp. 383-396.
326 Mikouchi T., Miyamoto M., Koizumi E., Makishima J., and McKay G. (2006) Relative burial
327 depths of nakhlites: An update. Lunar and Planetary Science Conference XXXVII, Abstract
328 #1865, Lunar Planet. Inst., Houston (CD-ROM).
329 Monders A.G., Médard E.**,** Grove T.L. (2007) Phase equilibrium investigations of the Adiron-
330 dack class basalts from the Gusev plains, Gusev crater, Mars. Meteoritics and Planetary Sci-
331 ences, 42, 131-148.
332 Musselwhite, D. S., H. A. Dalton, W. S. Kiefer, and A. H. Treiman (2006) Experimental petrol-
333 ogy of the basaltic shergottite Yamato-980459: Implications for the thermal structure of the
334 Martian mantle. Meteoritics and Planetary Science, 41, 1271-1290.

Myers, J.T., & Eugster, H.P. (1983) The system Fe-Si-O: Oxygen buffer calibrations to 1,500 K. Contributions to Mineralogy and Petrology, 82, 75-90.

Peslier A.H., Hnatyshin D., Herd, C.D.K., Walton E.L., Brandon A.D., Lapen T.J., Shafer J.T. (2010) Crystallization, melt inclusion, and redox history of a new Martian meteorite: olivine phyric shergottite LAR 06319. Geochimica et Cosmochimica Acta, 74, 4543-4576.

Righter K., Yang H., Costin G., and Downs R.T. (2008) Oxygen fugacity in the Martian mantle controlled by carbon: New constraints from the nakhlite MIL 03346. Meteoritics and Planetary Science, 43, 1709-1723.

Rutherford M. J. and Hammer J. E. (2008) Oxidation states in MIL 03346 nakhlite from experiments reproducing phenocryst-melt equilibria as a function of *f*O2 and T at 40–150 MPa. Lunar and Planetary Science Conference XXXIX, Abstract #1983, Lunar Planet. Inst., Houston (CD-ROM).

Sautter V., Barrat J. A., Jambon A., Lorand J. P., Gillet Ph., Javoy M., Joron J. L., and Lesourd M. (2002) A new Martian meteorite from Morocco: The nakhlite Northwest Africa 817. Earth and Planetary Science Letters, 195, 223–238.

Symes S. J. K., Borg L. E., Shearer C. K., and Irving A. J. (2008) The age of the Martian meteorite Northwest Africa 1195 and the differentiation history of the shergottites. Geochimica et Cosmochimica Acta, 72, 1696–1710.

Szymanski, A., Brenker, F. E., Palme, H., and El Goresy, A. (2010) High oxidation state during formation of Martian nakhlites. Meteoritics & Planetary Science, 45, 21-31.

Treiman A. H. and Irving A. J. (2008) Petrology of Martian meteorite Northwest Africa 998. Meteoritics and Planetary Science, 43, 829–854.

Treiman A. H. (2005) The nakhlite meteorites: Augite-rich igneous rocks from Mars. Chemie der Erde, 65, 203–270.

Treiman A.H. and Irving A.J. (2008) Petrology of the nakhlite (martian) meteorite Norwthwest Africa (NWA) 998. Meteoritics and Planetary Science, 43, 829-854.

Treiman A.H., Dyar M.D, McCanta M., Pieters C.M., Hiroi T., Lane M.D., and Bishop J. (2007) Martian dunite NWA 2737: Petrographic constraints geological history, shock events, and olivine color. Journal of Geophysical Research, 112, E04002, doi:10.1029/2006JE002777.

Turnock, A.C. and Eugster, H.P. (1962) Fe-Al Oxides: Phase Relationships Below 1000°C Journal of Petrology, 3, 533-565.

Ustinisik, G., Nekvasil, H., Lindsley, D. (2011) Differential degassing of H_2O, Cl, F, and S: Potential effects on lunar apatite. American Mineralogist, 96, 1650-1653.

Webster, J. D., R. J. Kinzler, and E. A. Mathez (1999) Chloride and Water Solubility in Basalt and Andesite Liquids and Implications for Magmatic Degassing. Geochimica et Cosmochimica Acta, 63, 729-738.

Figure Captions

Figure 1: (A) Backscattered electron (BSE) image of titanomagnetite (white, tmt), fayalite (light gray), and quenched assemblage (including glass and feldspathic phases) in the mesostasis of MIL 03346. The coarse-grained crystals enclosing the mesostasis are augite. (B) High magnification backscattered electron (BSE) image of titano-magnetite (light gray) showing the fine oxidation-driven exsolution lamellae of ilmenite (dark gray) in MIL 03346 ,106. (C) A FIB section was extracted from a region with many lamellae, with sample and stub indicated.

Figure 2: Ternary diagram showing the oxidation of the original titanomagnetite into magnetite and ilmenite. These are the measured compositions of the lamellae and host superimposed on the ternary which shows that the lamellae-host textures formed by oxidation. The tie line between ilmenite (green) and magnetite falls to the right of the original bulk composition (yellow) indicating an overall gain in Fe^{3+}, and thus oxidation; because the ilmenite contains essentially no Fe^{3+}, the remaining magnetite must contain more Fe^{3+} than the original titano-magnetite.

Figure 3: (A) Bright-field STEM image of the exsolution microstructure of ilmenite from the titano-magnetite host. Hercynite spinel (hrc) is present as a bright octahedron in the upper right quadrant of the image. (B) A high-resolution TEM image of a magnetite-ilmenite interface. The inset is a selected-area diffraction pattern showing the orientation relationship (0001) ilm ‖ (111) mag.

Figure 4: (A) Transmission electron microscope image of sub solidus oxidation-driven exsolution of ilmenite in magnetite. (B, C, D) Fe, Ti, and Al x-ray maps show another set of exsolution lamellae high in Al and Ti. A second set of very fine exsolution lamellae of spinel within magnetite are visible in the lower left portion of B, C, and D.

Figure 5: Temperature and fO_2 (relative to the fayalite-magnetite-quartz, or FMQ, buffer) for the MIL 03346 nakhlite magnetite-ilmenite pairs in this study, compared to those from previous studies. All temperatures and fO_2 calculated using the Ghiorso and Evans (2008) oxy-barometer. All temperatures and fO_2 from the literature nakhlites were calculated using data from Reid and Bunch (1975), Treiman and Irving (2008), Szymanski et al. (2010), Sautter et al. (2002), and Boctor et al. (1976). Hercynite exsolution line is estimated from the Fe_3O_4-$FeAl_2O_4$ system (Turner and Eugster, 1962). Hercynite presence (~550 ºC) and magnetite-ilmenite exsolution (< 350 ºC) are both lower temperature events than recorded in nakhlites from the literature. FMQ buffer is that determined by Myers and Eugster (1983).

Figure 6: Combined T-fO_2 estimates from previous studies (Rutherford and Hammer, 2008; McCanta et al., 2009; Righter et al., 2008) with our calculations for nakhlites, which highlights an early oxidation trend followed by later reduction recorded in the nakhlites, and finally an oxidation event at low temperatures. The latter oxidation trend is discussed in Figure 5 and in the text. The McCanta et al. (2009) estimate of FMQ-0.3 is not shown because temperature was not calculated in that study, but the high FMQ value is consistent with this scenario as well.

411

412 **Table 1: Titanomagnetite, and magnetite and ilmenite analyses**
413 **and temperature and fO_2 calculations**
414

	Titanomagnetite host [a]	Magnetite lamellae [b]	Ilmenite lamellae [b]
SiO_2	0.30	-	-
TiO_2	15.39	3.87	52.6
Al_2O_3	3.06	2.92	n.d.
V_2O_3	0.37	-	-
FeO (tot)	75.34	87.4	45.9
MnO	0.55	0.41	1.40
MgO	0.09	<0.03	0.10
CaO	0.03	-	-
Total	95.13	94.32	100
FeO	46.78	36.52	45.93
Fe_2O_3	31.74	56.54	0.01
Recalc. total	98.30	99.98	99.91
Mg/Mn		<0.128	0.126
T(ºC) (GE08)		228	
$logfO_2$		-52.05	
Δ FMQ		-9.00	
T(ºC) (GS91)		203	
$logfO_2$		-51.84	
Δ FMQ		-8.78	

415 a Typical titano-magnetite host microprobe analysis from Day et al. (2006)

416 b Counting statistics errors on the EDX analyses are < 1% on major elements, a ~2 % on minor elements

417 n.d. = not detected; GE08 = Ghiorso and Evans (2008); GS91 = Ghiorso and Sack (1991)

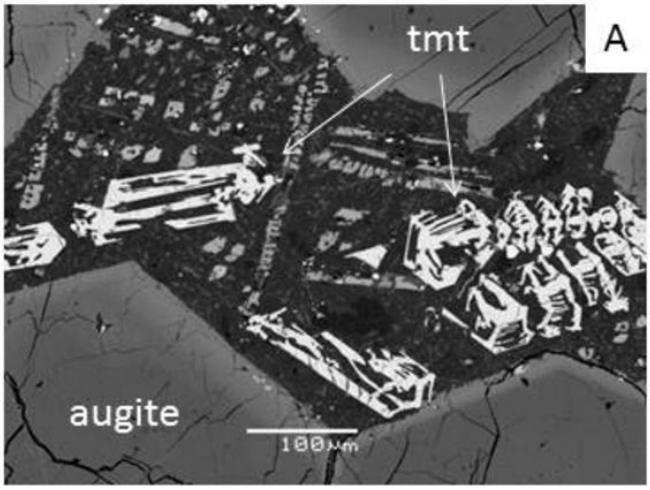
tmt
A
augite
100 µm

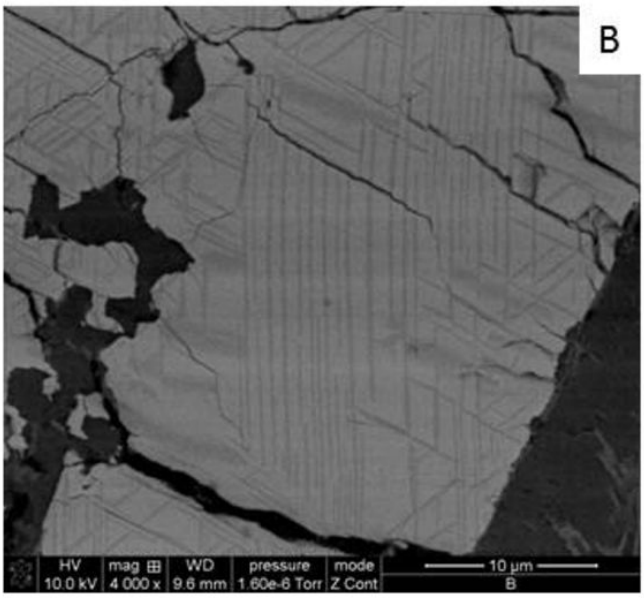
B
HV
10.0 kV
mag
4 000 x
WD
9.6 mm
pressure
1.60e-6 Torr
mode
Z Cont
10 µm
B

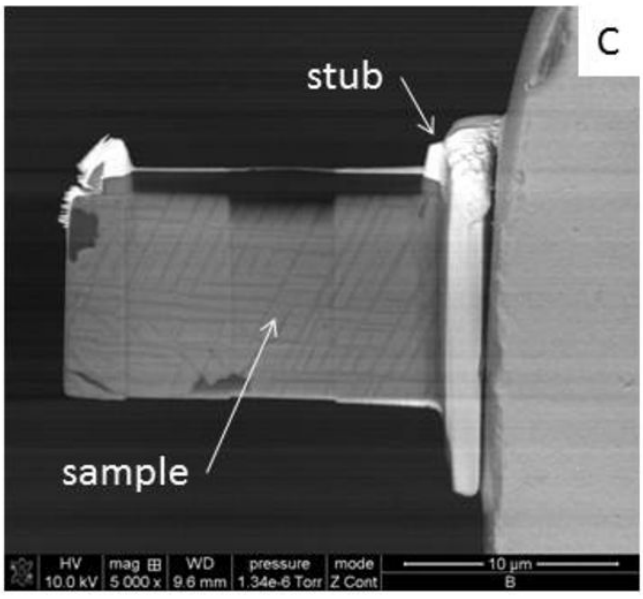
C
stub
sample
HV
10.0 kV
mag
5 000 x
WD
9.6 mm
pressure
1.34e-6 Torr
mode
Z Cont
10 µm
B

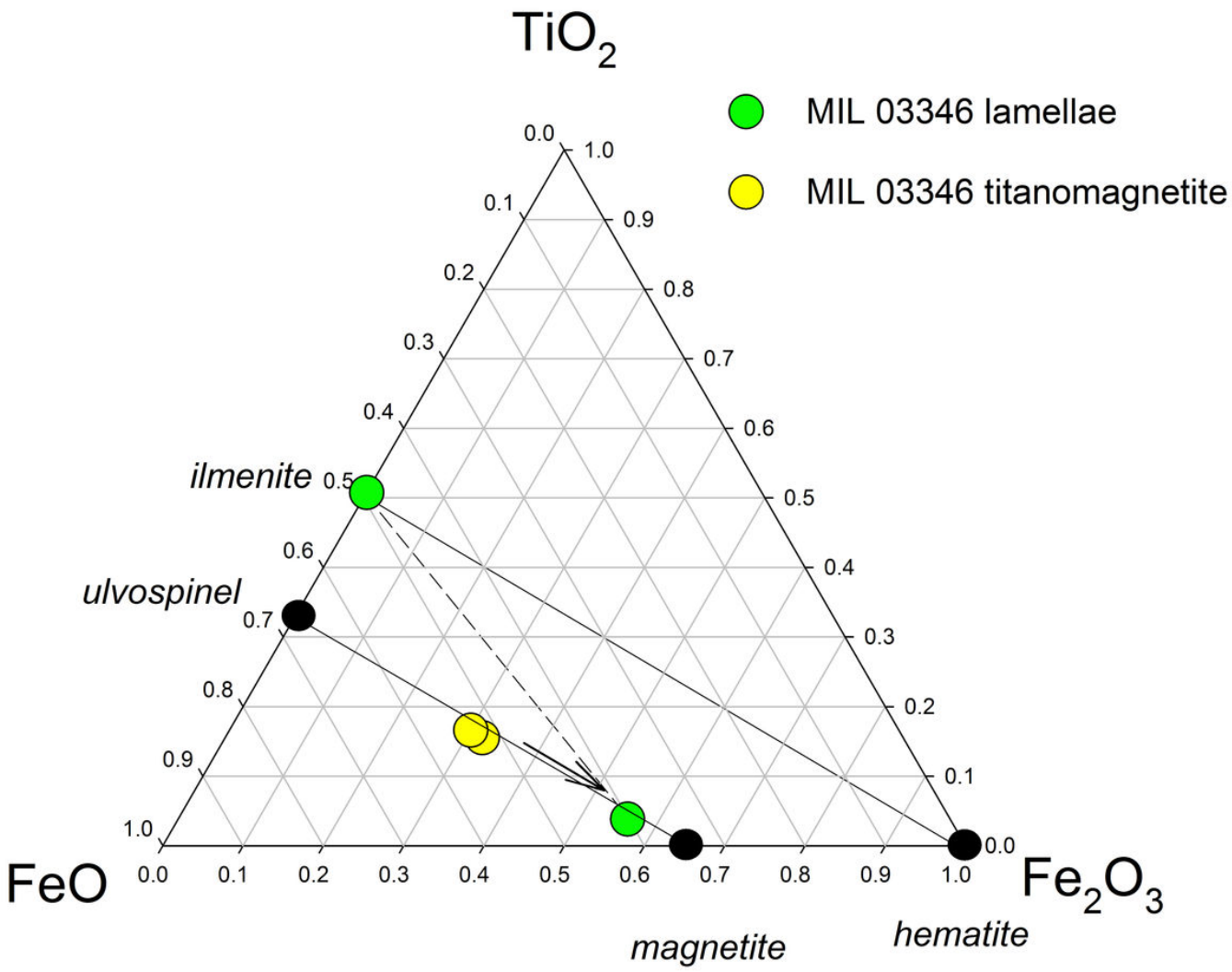
TiO2
MIL 03346 lamellae
MIL 03346 titanomagnetite
ilmenite
ulvospinel
magnetite
hematite
FeO
Fe2O3
0.0
0.1
0.2
0.3
0.4
0.5
0.6
0.7
0.8
0.9
1.0

This is a preprint, the final version is subject to change, of the American Mineralogist (MSA)
Cite as Authors (Year) Title. American Mineralogist, in press.
(DOI will not work until issue is live.) DOI: http://dx.doi.org/10.2138/am-2014-4926

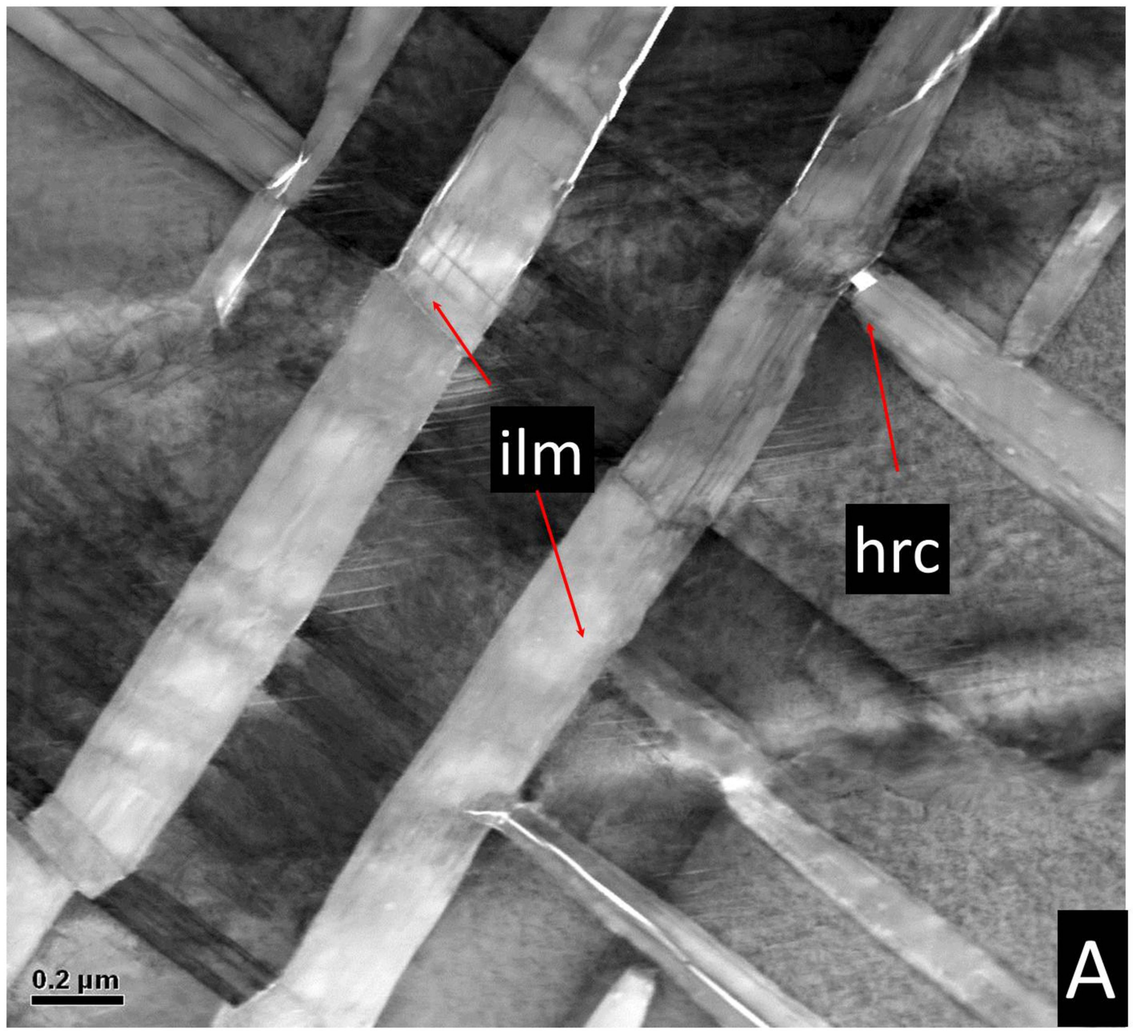

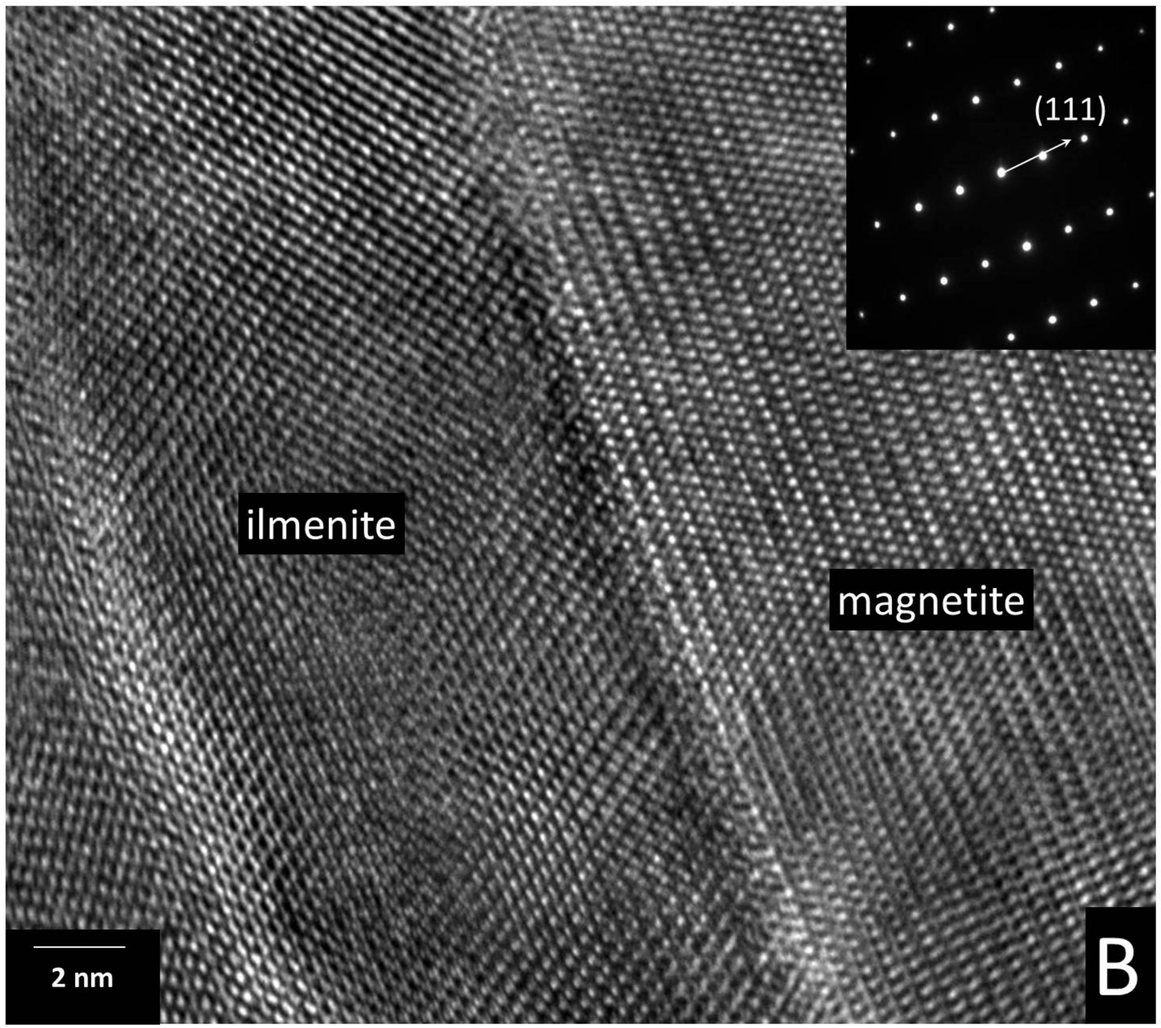

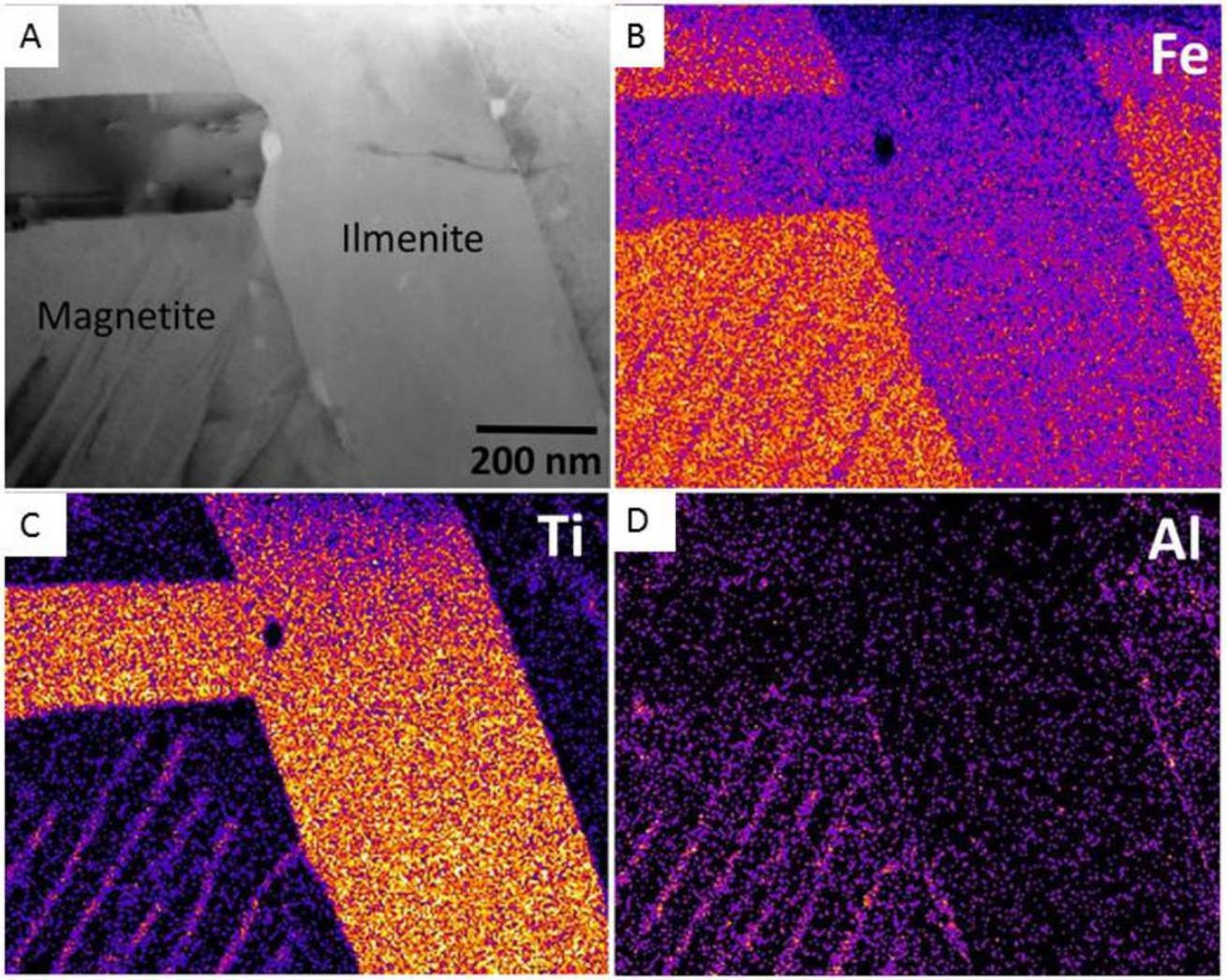
A
Ilmenite
Magnetite
200 nm
B
Fe
C
Ti
D
Al

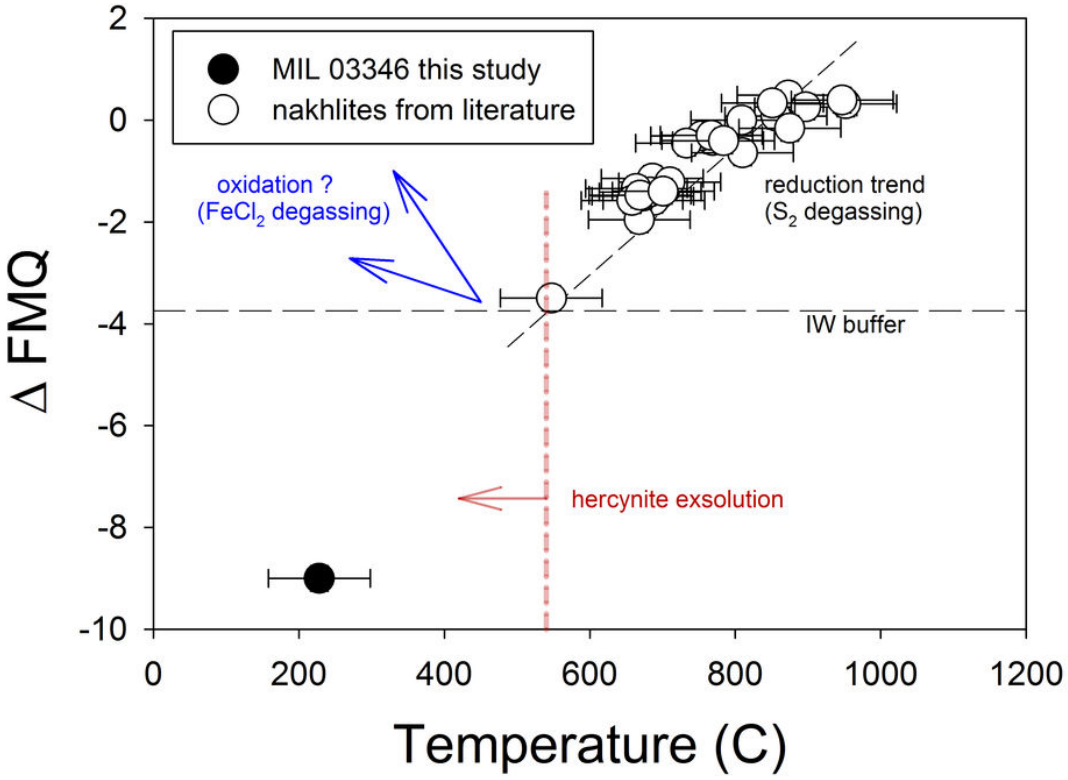
MIL 03346 this study
nakhlites from literature
oxidation ?
(FeCl2 degassing)
reduction trend
(S2 degassing)
IW buffer
hercynite exsolution
Δ FMQ
Temperature (C)
2
0
-2
-4
-6
-8
-10
0
200
400
600
800
1000
1200

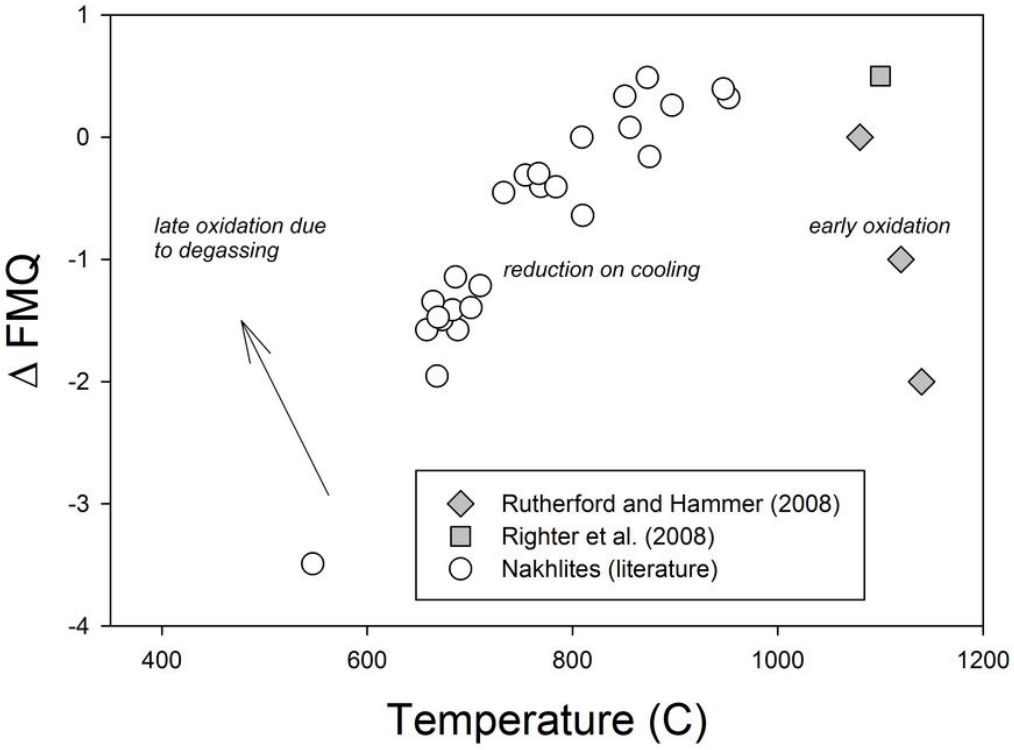
1
0
-1
-2
-3
-4
Δ FMQ
400
600
800
1000
1200
Temperature (C)
late oxidation due
to degassing
reduction on cooling
early oxidation
Rutherford and Hammer (2008)
Righter et al. (2008)
Nakhlites (literature)